Available online at www.sciencedirect.com
SCIENCE DIRECT®
Journal of Catalysis 227 (2004) 11–25
JOURNAL OF CATALYSIS
www.elsevier.com/locate/jcat

Characterization and catalytic activity of differently pretreated Pd/Al_2O_3 catalysts: the role of acid sites and of palladium–alumina interactions

M. Skotak [a], Z. Karpiński [a,b,*], W. Juszczyk [a], J. Pielaszek [a], L. Kępiński [c], D.V. Kazachkin [d], V.I. Kovalchuk [d], J.L. d'Itri [d]

[a] *Institute of Physical Chemistry, Polish Academy of Sciences, ul. Kasprzaka 44/52, PL-01 224 Warsaw, Poland*
[b] *Faculty of Mathematics and Natural Sciences, Cardinal Stefan Wyszyński University, ul. Dewajtis 5, PL-01 815 Warsaw, Poland*
[c] *Institute of Low Temperature and Structure Research, Polish Academy of Sciences, PO Box 937, PL-50 950 Wrocław, Poland*
[d] *Department of Chemical and Petroleum Engineering, University of Pittsburgh, PA 15261, USA*

Received 1 April 2004; revised 24 May 2004; accepted 5 June 2004

Available online 20 July 2004

Abstract

The effect of catalyst pretreatment on the performance of chlorine-free γ-alumina-supported palladium catalysts with metal loadings in the range of 0.3 to 2.77 wt% has been investigated in the hydroconversion of *n*-hexane (nH) and 2,2-dimethylbutane (22DMB) at 290 °C and atmospheric pressure. The catalyst properties were modified by varying the catalyst pretreatment: low-temperature reduction (LTR) at 300 °C; high-temperature reduction (HTR) at 600 °C; and oxidation of highly reduced catalysts followed by LTR (regeneration). The isomerization activity for both nH and 22DMB conversion is enhanced by HTR of the Pd/Al_2O_3 as compared to LTR and regeneration. It is concluded that HTR increases the Lewis acidity of the alumina and the participation of Lewis acid sites improves catalytic performance. The influence of Lewis acid catalyst sites on the macroscopic kinetics overshadows the modest catalytic contribution from palladium. Ammonia effectively blocks the acid centers and limits the overall catalytic performance to metal-only catalysis. The role of support acid sites in the conversion of C_6-hydrocarbons was further demonstrated by isomerization activity associated with 22DMB hydroconversion catalyzed by an alumina-supported Ni catalyst. Based on the results of FTIR studies of adsorbed CO and results of temperature-programmed palladium hydride phase decomposition (TPHD), it was concluded that a part of the alumina-supported Pd transforms into a Pd–Al alloy during the HTR pretreatment. The catalytic performance of the regenerated catalysts in the C_6-alkane conversion is consistent with the suggestion that the Pd–Al alloy formed during HTR decomposes during the regeneration treatment to form Al_2O_3 moieties on the Pd surface. These moieties, most likely, interact strongly with nearby palladium species, creating sites which are active for alkane isomerization and, simultaneously, resistant to coking.

Keywords: Pd/Al_2O_3 catalysts; *n*-Hexane conversion; 2,2-Dimethylbutane conversion; High-temperature reduction; IR spectroscopy of adsorbed CO; Role of acid sites of alumina; Temperature-programmed hydride decomposition; Palladium–alumina interactions

1. Introduction

The catalytic performance of alumina-supported palladium for alkane hydroconversion is affected significantly by the catalyst pretreatment conditions [1–5]. For example, when Pd/Al_2O_3 is prereduced at 600 °C, the overall activity increases and the isomerization selectivity is enhanced to 95% for the hydroconversion of C_6-alkanes at reaction temperatures less than 300 °C in comparison with catalysts prereduced at temperatures less than 400 °C [3–5]. The enhanced isomerization selectivity was attributed to an increase in the Lewis acidity of the γ-alumina that results from the high-temperature pretreatment [6,7]. Confirmation

* Corresponding author. Fax: +48 22 6325276.
E-mail address: zk@ichf.edu.pl (Z. Karpiński).

0021-9517/$ – see front matter
doi:10.1016/j.jcat.2004.06.007

of the stronger acidity of Pd/Al_2O_3 catalysts subjected to high-temperature reduction was provided via temperature-programmed desorption (TPD) experiments with various bases such as ammonia [4], pyridyne [5], and triethylamine [8].

Whereas previous work focused on the evolution of support acidity, much less attention has been paid to the state of the metal phase in the Pd/Al_2O_3 catalysts prereduced at high temperature (HTR state). The role of Pd has commonly been described as to catalyze the dissociation of hydrogen to supply H atoms required for hydrogenative desorption of rearranged alkyl fragments from acid sites of γ-alumina [2–5]. However, under conditions of low support acidity, the metal may play a dominative role. For example, when a Pd/Al_2O_3 catalyst prereduced at high temperature is regenerated by oxidation and then by reduction at 300 °C, the isomerization selectivity is much higher than when it is prereduced at low temperatures (LTR state) [4]. If "regeneration" greatly reduces the acidity of alumina (acquired during HTR), the catalytic performance of the regenerated sample should be associated with the metal. And metal properties such as particle morphology and electronic state may change during the pretreatment cycle: LTR–HTR–regeneration. An understanding of the metal state and its influence on the catalytic behavior of the regenerated samples is still lacking.

The objective of the present investigation was to provide further insight into the role of the metal and the acid sites of alumina-supported Pd catalysts for the reactions of *n*-hexane (nH) and 2,2-dimethylbutane (22DMB) hydroconversion. Catalysts with varying metal loadings were subjected to different pretreatment conditions to modify the morphology of metallic particles and the acidity of the support. In contrast to the samples reduced at low temperature, the highly reduced catalysts demonstrated much more stable activity as a function of time on stream [2,4]. In the present work the amount and the morphology of strongly retained carbonaceous deposits after alkane conversion were compared for differently pretreated Pd catalysts.

The support acidity and morphology of Pd particles were probed by the FTIR spectroscopy of adsorbed CO. Because CO is a weak base, it interacts with the strongest Lewis acid sites that may possess the highest catalytic activity for alkane conversion. As well, NH_3 was used to block the acid sites of alumina activated by high-temperature reduction (HTR). Ammonia desorbs from Pd during gradual heating before reaching 290 °C, the reaction temperature of alkane conversion [9], whereas NH_3 will still block acid sites of alumina [4,10]. Also, the role of the support Lewis acidity was probed using alumina-supported Ni, which normally exhibits negligible isomerization activity in the 22DMB reaction [11–14].

2. Experimental methods

2.1. Catalyst preparation and characterization

The catalyst support was γ-Al_2O_3 (Alumina Shell S618; chemical composition Al_2O_3—98.5 wt%, H_2O—1.5 wt%; 240 m^2/g surface area; 0.8 cm^3/g pore volume; 75–120 mesh). It was washed with diluted nitric acid and rinsed thoroughly with redistilled water. Four Pd/Al_2O_3 catalysts with metal loadings in the range 0.3–2.77 wt% Pd were prepared by impregnation of the support with solutions of palladium acetylacetonate (99.8%, Alfa Produkte, Karlsruhe, Germany) in benzene (analytical grade from POCh, Gliwice, Poland) according to the procedure of Boitiaux et al. [15]. After impregnation and drying in an oven at 80 °C in air for 12 h, the catalysts were precalcined at 350 °C in flowing air (∼ 400 cm^3/min), reduced in H_2 (∼ 250 cm^3/min) at 200 °C for 0.25 h under fluidized bed conditions, cooled in flowing He (∼ 250 cm^3/min) to ambient temperature, transferred to glass-stoppered bottles, and stored in a desiccator. The Ni/Al_2O_3 catalyst was prepared by incipient wetness impregnation of the support with an aqueous solution of nickel nitrate (analytical grade, POCh, Gliwice, Poland) and handled the same way as the Pd catalysts. The catalyst compositions are listed in Table 1. Before use, the catalyst samples were pretreated via three different protocols, as described in Table 1.

The metal dispersion was determined from pulse H_2 chemisorption experiments conducted at 70 °C; the adsorption stoichiometry (expressed as H_{ad}/Pd_s) was assumed to be 1. After the chemisorption measurements the catalysts were cooled to room temperature under a 10% H_2/Ar mixture flow (25 cm^3/min), and the temperature-programmed palladium hydride decomposition (TPHD) was conducted following a previously reported procedure [16]. All gases used (H_2, Ar, He, 10% H_2/Ar) were of research grade purity and were passed through MnO/SiO_2 traps to remove traces of O_2.

The X-ray diffraction (XRD) patterns were obtained with a standard Rigaku–Denki diffractometer equipped with a Ni-filtered Cu$K\alpha$ radiation source. The Pd/Al_2O_3 catalysts were scanned, step by step, at 2θ intervals of 0.05°; counts were collected for 10 s at each step. The metal crystallite size was calculated from the Scherrer equation using the Pd(111) reflection after correction for the contribution from Al_2O_3.

The high-resolution transmission electron microscopy (HRTEM) and selected area diffraction (SEAD) images were recorded with a Philips CM20 SuperTwin microscope. The point resolution was 0.25 nm when operated at 200 kV. The specimens for HRTEM were prepared by dispersing the powdered samples in methanol and placing a droplet of the suspension onto a copper microscope grid covered with perforated carbon. The Pd particles on the alumina support were identified in the HRTEM images using Pd(111) lattice fringes (0.225 nm) measured by the fast Fourier transform (FFT) method (the line resolution was 0.15 nm).

Table 1
Catalyst composition and results of routine characterization

Pd loading (wt%)	Pretreatment[a]	Metal particle size, nm			Pd dispersion[b] (D) (%)	H/Pd_{bulk} from β-hydride decomposition
		d_{XRD}[c]	d_{TEM}	d_{chem}[d]		
0.3	LTR	[e]	[e]	4.9	23	0.01
	HTR	[e]	[e]	560	0.2	0.13
	Regeneration	[e]	[e]	112	1	0.07
0.6	LTR	[e]	[e]	2.9	39	0.03
	HTR	3.5	4.6[f]	66	1.7	0.28
	Regeneration	3.0	[e]	8.6	13	0.20
1.46	LTR	3.3	[e]	3.9	29	0.46
	HTR	3.9	[e]	11.8	9.5	0.41
	Regeneration	3.3	[e]	7.5	15	0.41
2.77	LTR	2.8	4.8[g]	3.7	30	0.61
	HTR	4.0	4.8[h]	5.9	19	0.52
	Regeneration	3.5	4.0[i]	9.3	12	0.51

[a] LTR (low-temperature reduction) consisted of precalcination of a fresh catalyst sample under O_2 flow at 400 °C for 1 h followed by purging with a He flow for 5 min and subsequent reduction in a H_2 flow at 300 °C for 1 h; HTR (high-temperature reduction) included oxidation of the LTR sample with an O_2 flow at 300 °C for 0.5 h followed by purging with a He flow for 5 min, and subsequent reduction in a H_2 flow at 600 °C for 17 h, followed by purging with a He flow at 600 °C for 1 h; regeneration pretreatment consisted of oxidation of the HTR sample in an O_2 flow at 500 °C for 1 h followed by purging with a He flow for 5 min and reduction in a H_2 flow at 300 °C for 1 h.
[b] Based on hydrogen chemisorption at 70 °C.
[c] Calculated with the Scherrer equation using (111) reflection, after subtracting background from Al_2O_3.
[d] Calculated as 112/D [57].
[e] Too low signal or not measured.
[f] Average value from 14 particles.
[g] Average value from 26 particles.
[h] Average value from 40 particles.
[i] Average value from 43 particles.

2.2. Catalytic conversions of n-hexane (nH) and 2,2-dimethylbutane (22DMB)

The catalytic conversions of nH (> 99.9%, Chemipan, Poland) and 22DMB (puriss., Fluka AG) in excess H_2 (research grade, additionally purified using a MnO/SiO_2 trap) were conducted in a continuous-flow reaction system under atmospheric pressure, as described previously [2–5]. Briefly, a tubular fused silica reactor equipped with a fritted disk was loaded with Pd/Al_2O_3 catalyst. The amount of catalyst was varied in the range of 0.15–0.25 g in order to keep conversion below 15%. Prior to reaction, the catalyst was subjected to one of the pretreatments (LTR, HTR, and regeneration; see Table 1). Then the sample was cooled to the reaction temperature in an H_2 flow. When NH_3 was used to block the acid sites of selected catalysts, the HTR-pretreated sample was exposed to a flow of NH_3 (Merck–Schuchardt, purity 99.96%) (1 cm^3/min) and He (25 cm^3/min) at 100 °C for 40 min and then purged with a He flow (25 cm^3/min) for ∼ 0.5 h to remove weakly bound NH_3 [4]. Then, the sample was heated to the reaction temperature (290 °C) in a flow of 25% H_2 in He (33 cm^3/min).

The start of the kinetics experiment consisted of flowing a H_2 stream (8.0 cm^3/min) through a saturator with C_6-alkane maintained at 0 °C for nH and at −15 °C for 22DMB. The saturator conditions provided a partial pressure of 45 Torr for nH and 51.5 Torr for 22DMB. The reactor effluent was analyzed using an on-line GC (HP 5890 Series II with FID) equipped with a 50 m PONA, #19091S-001-HP, capillary column. Except for the HTR samples, the Pd/Al_2O_3 catalysts deactivated with TOS losing ∼ 30–40% of the initial activity [4], and steady-state conversions were achieved after ∼ 2–2.5 h on stream. Afterwards, the reaction temperature was decreased at increments of 10–20 °C, and the steady-state conversion and the product selectivities were measured at each temperature. For all LTR and regenerated samples, the steady-state conversion was < 5% at the highest reaction temperature. For the HTR samples, the conversion was as high as ∼ 15% at the highest reaction temperature. Blank experiments with differently pretreated metal-free γ-Al_2O_3 showed negligible activity at temperatures below 300 °C. The product selectivities were calculated as the carbon percentage of nH (or 22DMB) incorporated in a designated product.

A 5 wt% Ni/Al_2O_3 catalyst pretreated according to the LTR, HTR, and regeneration protocols was also tested in the reaction of 22DMB hydroconversion at 280 °C to elucidate the role of alumina acid sites in low-temperature alkane catalysis. As Ni is much more active than Pd in alkane-conversion reactions, it was necessary to use 0.0019 g of the 5 wt% Ni/Al_2O_3 catalyst diluted with 0.2536 g of Al_2O_3 to keep the alkane conversion at a reasonably low level and the concentration of acid sites at a level similar to that for Pd catalysts.

2.3. Temperature-programmed oxidation

Several different samples were tested in ∼ 0.2 g amounts: metal-free Al_2O_3 (pretreated by the three different methods) and 0.3 wt% Pd/Al_2O_3, 0.6 wt% Pd/Al_2O_3, 1.46 wt% Pd/Al_2O_3, 2.77 wt% Pd/Al_2O_3, and 1.1 wt% Pd/SiO_2 catalysts. After either nH or 22DMB hydroconversion at 290 °C for 2.5 h, the samples were purged with Ar at 290 °C for 5 min, cooled to room temperature in Ar, and sealed by closing two reactor stopcocks. Then the reactor (U-tube, fused silica) was attached to the TPD system and flushed with He. The temperature-programmed oxidation (TPO) experiments were conducted by flowing 25 cm^3/min of 1% O_2 in He (controlled by a Bronkhorst Hi-Tec mass-flow controller) while heating at 10 °C/min from room temperature to ∼ 600 °C using an Omega 2011 temperature controller. The outlet of the reactor containing the catalyst sample was connected via a Tee union to a 2-m capillary leading to the sampling valve (Balzers) of a quadrupole mass spectrometer (Dycor M200, Ametek) and vent. All parts between the reactor outlet and the mass spectrometer were heated to 100 °C. The temperature and mass signal of released CO_2 (m/z 44) were monitored at 15-s intervals.

2.4. FTIR study of adsorbed CO

The infrared spectra were recorded with a Research Series II FTIR spectrometer (Mattson) equipped with a liquid N_2 cooled MCT detector. The IR cell was similar to that described elsewhere [17]. The cell was equipped with glass stopcocks connected to gas inlet/outlet ports and to a vacuum port with a turbomolecular pump (Leybold, 2000 l s^{-1}). The spectra were measured in the range of 1000–4000 cm^{-1} with a resolution of 4 cm^{-1} and 64 scans were accumulated per spectrum.

The infrared spectra were collected in the transmission mode, which mandates the use of thin wafers of the catalyst sample. The self-supporting wafers (28–35 mg/cm^2 thick) were prepared by powdering the catalyst material in an agate mortar and then pressing the powder at 50 MPa for 1 min. The catalyst wafer was placed into the quartz sample holder of the IR cell, and the system was evacuated to a pressure less than 10^{-6} Torr (measured with a MKS-Baratron gauge). Then the wafer was pretreated using 10% O_2 in He (Liquid Carbonics, 99.999%) and 5% H_2 in Ar (PraxAir, 99.999%) according to the LTR, HTR, and regeneration procedures specified in Table 1. Each pretreatment was followed by the FTIR study of the adsorbed CO, and all FTIR experiments for a given catalyst were done with the same wafer.

The carbon monoxide (PraxAir, 99.99%) adsorption on a pretreated catalyst wafer was performed in several steps. After the catalyst was pretreated and evacuated for 0.5 h at the last pretreatment temperature, it was cooled to room temperature in vacuum. Ten Torr CO was introduced into the IR unit and 10 min later an IR spectrum was recorded. Next, the cell was evacuated for 10 min and a new IR spectrum recorded. After a second 10-min evacuation, 80 Torr of CO was introduced, and the cell was allowed to equilibrate for 16 h. Afterwards a new spectrum was recorded. Finally, the cell was evacuated for 10 min, and the last spectrum was recorded. The same CO adsorption procedure was used by Marchese et al. [18] to identify acid sites in γ-Al_2O_3.

3. Results

3.1. Palladium particle size in differently pretreated Pd/Al_2O_3

The metal particle sizes for the catalysts based on H_2 chemisorption measurements, XRD, and TEM investigations are shown in Table 1. The metal dispersions determined by H_2 chemisorption were in the range of 23–39% for the LTR samples. The H_2 uptake decreased substantially for the HTR and the regeneration samples in comparison with the LTR samples. The small uptake is consistent with a low metal surface area. However, a decrease in the metal surface area for the HTR and regenerated samples was not confirmed by XRD and/or TEM studies for the higher metal loading samples. The XRD and TEM results showed that the average Pd particle size for the 1.46 and 2.77 wt% Pd/Al_2O_3 catalysts did not vary significantly after the three different pretreatments (Table 1). The very small hydrogen uptakes measured for the HTR samples of 0.3 wt% Pd/Al_2O_3 catalyst were discussed in detail in Ref. [4] and, thus, will not be considered further in the present work.

3.2. Catalytic conversions of nH and 22DMB

The steady-state kinetics results are presented both as moles reacted C_6-alkane per g_{Pd} per second (Fig. 1) and as turnover frequencies based on the H_2 chemisorption data (Table 2). For the Pd/Al_2O_3 catalysts pretreated according to the LTR protocol, both the catalytic activity and the isomerization selectivity were quite low (Fig. 1). However, the HTR pretreatment resulted in an order of magnitude increase in catalytic activity as compared to the LTR samples. The increase in activity was accompanied by a dramatic increase in the isomerization selectivity from 20–55% to 93–96% (Fig. 1).

Regeneration of the HTR-pretreated Pd/Al_2O_3 samples decreased the catalytic activity to a level comparable to that of the LTR-pretreated samples. However, the isomerization selectivities were in the range of 78–94% for samples used in the 22DMB reaction and 48–68% for samples used in the nH reaction. It is also worth noting that the catalytic activity of the HTR and regenerated samples decreased with increasing Pd loading. In general, the activities of Pd/Al_2O_3 catalysts were higher for 22DMB conversion than for nH conversion (Fig. 1). This activity difference will not be discussed further in the present work. It may result from more extensive

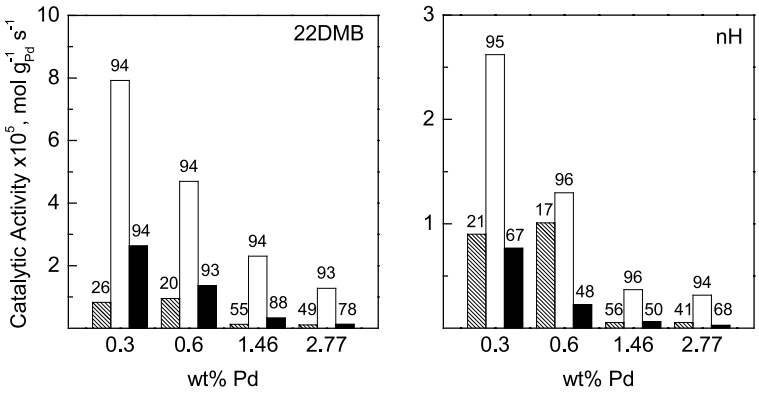

Fig. 1. Activity of Pd/Al_2O_3 catalysts subjected to the LTR (the hatched bars), HTR (the empty bars), and regeneration (the filled bars) pretreatments in nH and 22DMB hydroconversion at 290 °C. Numbers above bars indicate the selectivity (%) toward isomerization (for the 22DMB hydroconversion) or toward C_6-product formation (for the nH hydroconversion). The more detailed product distribution was reported earlier [4].

Table 2
Turnover frequencies for hydrogenolysis ($TOF_{<C6}$), isomerization (TOF_{is}), and cyclization (TOF_{cycl}) in *n*-hexane and 2,2-dimethylbutane conversions at 290 °C catalyzed by Pd/Al_2O_3

Catalyst (Pd loading)	nH reaction			22DMB reaction	
pretreatment[a]	$TOF_{<C6}$ (s^{-1})	TOF_{is} (s^{-1})	TOF^{b}_{cycl} (s^{-1})	$TOF_{<C6}$ (s^{-1})	TOF_{is} (s^{-1})
0.3 wt%					
LTR	3.19E–3	4.1E–4	4.6E–4	1.89E–3	1.80E–3
HTR	7.40E–2	1.24E0	5.76E–2	2.64E–1	3.86E0
Regeneration	2.60E–2	4.94E–2	3.89E–3	5.92E–2	2.15E–1
0.6 wt%					
LTR	2.25E–3	2.2E–4	2.2E–4	2.02E–3	5.0E–4
HTR	3.47E–3	7.12E–2	2.47E–3	1.56E–2	2.63E–1
Regeneration	2.87E–3	1.99E–3	6.1E–4	8.1E–4	1.01E–2
1.46 wt%					
LTR	8E–5	4E–5	7E–5	3.0E–4	1.1E–4
HTR	1.8E–4	3.60E–3	1.9E–4	1.43E–3	2.37E–2
Regeneration	1.9E–4	1.0E–4	9E–5	1.8E–4	1.98E–3
2.77 wt%					
LTR	9E–5	2E–5	4E–5	2.6E–4	9E–5
HTR	1.1E–4	1.50E–3	8E–5	4.0E–4	6.56E–3
Regeneration	5E–5	4.0E–5	7E–5	6E–5	1.02E–3

[a] See Table 1 for pretreatment code.
[b] Methylcyclopentane (major product), cyclohexane, and benzene were the cyclization products.

coking during the nH reaction (vide infra); however, further experimentation is required.

Adsorption of NH_3 on the HTR-pretreated 0.3 wt% Pd/Al_2O_3 and 2.77 wt% Pd/Al_2O_3 catalysts suppressed the catalytic activity for 22DMB hydroconversion by two orders of magnitude as compared to the HTR samples without NH_3 treatment (Fig. 2). The activities were even lower than those for the LTR samples. The NH_3 adsorption also decreased the isomerization selectivity of the HTR-pretreated 0.3 wt% Pd/Al_2O_3 and 2.77 wt% Pd/Al_2O_3 from 94 and 93% to 71 and 59%, respectively. The selectivities for the NH_3-pretreated samples were still higher than those of the LTR-pretreated samples (26 and 49% for the 0.3 wt% Pd/Al_2O_3 and 2.77 wt% Pd/Al_2O_3 catalysts, respectively).

The HTR treatment of the 5 wt% Ni/Al_2O_3 catalyst resulted in an isomerization selectivity as high as ∼ 7%, whereas the LTR-pretreated and regenerated samples did not catalyze isomerization reactions (Fig. 3). It is important to note that Ni itself exhibits negligible isomerization activity [11–14]. The activity trend for the differently pretreated Ni/Al_2O_3 catalysts was similar to that of Pd/Al_2O_3; the 22DMB conversion was the highest for the HTR-pretreated sample and the lowest for the LTR-pretreated Ni catalyst.

3.3. *Temperature-programmed oxidation study of Pd/Al_2O_3 catalysts after C_6-alkane conversion*

Carbon dioxide formed during TPO of the Pd/Al_2O_3 catalysts used for the hydroconversion of nH or 22DMB for ∼ 2.5 h (Fig. 4). For all samples the carbon-to-surface-Pd-atom (C/Pd_s) ratios were typically less than 0.1. Such low C/Pd_s levels do not merit extensive interpretation because of the large experimental error. However, it would not be unreasonable to consider this carbon as "irreversible" carbon

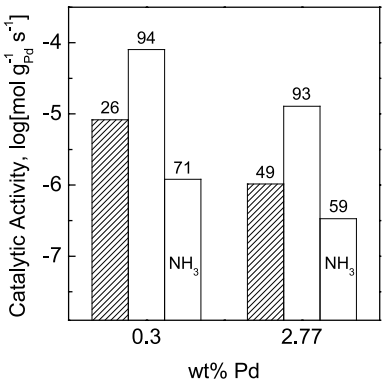

Fig. 2. The effect of NH_3 adsorption on the behavior of the highly reduced 0.3 wt% Pd/Al_2O_3 and 2.77 wt% Pd/Al_2O_3 catalysts in 22DMB conversion at 290 °C. The respective results for the LTR (hatched bars) and HTR (empty bars) samples without NH_3 poisoning are also shown for comparison. Numbers above the bars indicate the selectivity (%) toward isomerization.

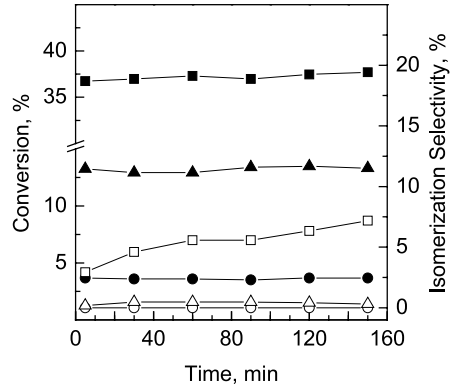

Fig. 3. Time-on-stream performance of the LTR (circles), HTR (squares), and regenerated (triangles) Ni/Al_2O_3 samples diluted with the metal free support (0.0019 g of 5 wt% Ni/Al_2O_3 + 0.2536 g of Al_2O_3) in the 22DMB hydroconversion at 280 °C. Filled symbols denote the degree of conversion, empty symbols isomerization selectivity.

that is in the form of highly dehydrogenated and irreversibly adsorbed species [19]. Similar C/Pt_s ratios for "irreversible" carbon were reported by Garin et al. [19].

In general, a larger amount of CO_2 evolved during TPO after nH conversion reaction than after 22DMB. For both reactions the trend observed for the amount of CO_2 evolved was LTR-pretreated samples > HTR-pretreated samples ≫ regenerated samples. There was also a small shift toward

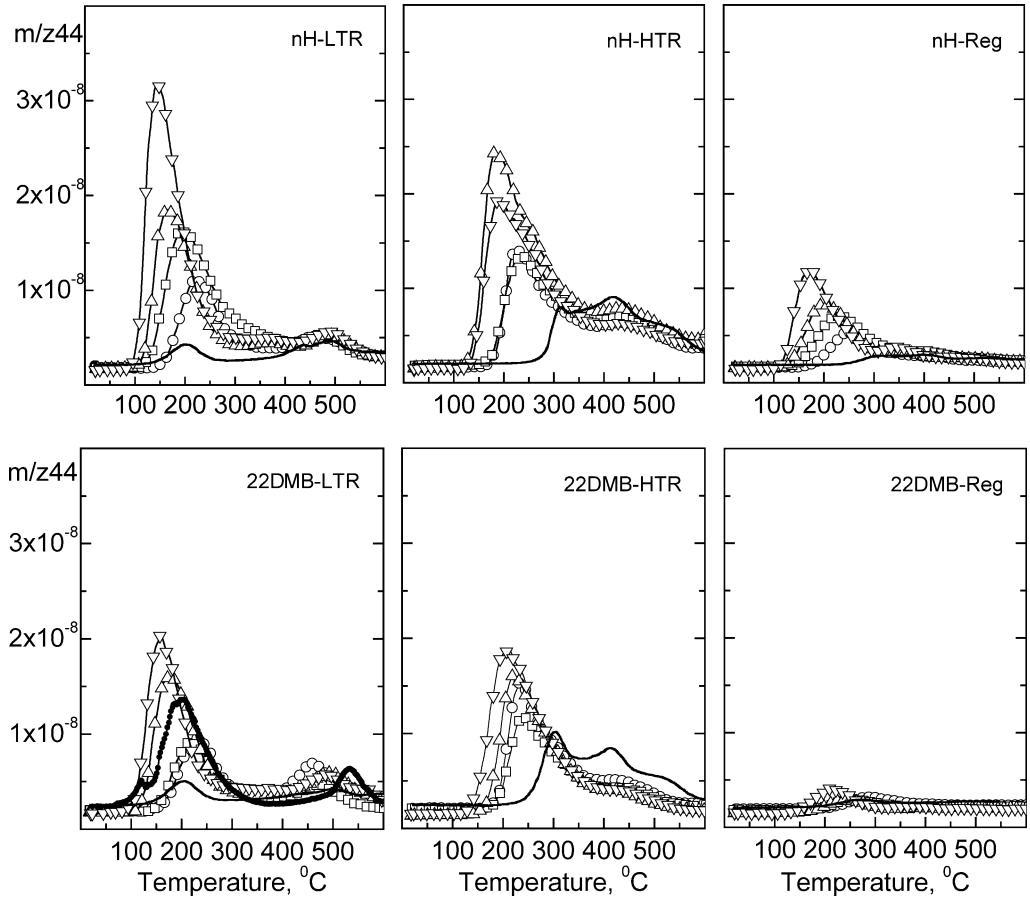

Fig. 4. TPO profiles of the differently pretreated 0.3 wt% Pd/Al_2O_3 (○), 0.6 wt% Pd/Al_2O_3 (□), 1.46 wt% Pd/Al_2O_3 (△), 2.77 wt% Pd/Al_2O_3 (▽), and 1.1 wt% Pd/SiO_2 (●) catalysts after *n*-hexane (nH) and 2,2-dimethylbutane (22DMB) reactions. Solid lines without symbols represent TPO profiles from differently pretreated γ-Al_2O_3 subjected to nH and 22DMB conversions.

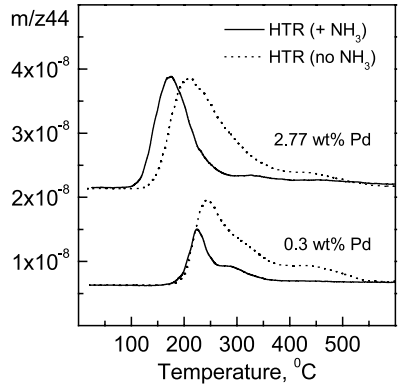

Fig. 5. TPO profiles of the NH_3-pretreated (solid line) HTR 0.3 wt% Pd/Al_2O_3 and 2.77 wt% Pd/Al_2O_3 catalysts after 22DMB conversion. TPO profiles of the HTR samples without NH_3 poisoning (dashed line) are included for comparison.

higher temperatures for CO_2 evolution from the HTR samples in comparison to the LTR and regenerated catalysts (Fig. 4). On a per-gram basis there was a correlation between amount of CO_2 formed and metal loading: 2.77 wt% Pd/Al_2O_3 > 1.46 wt% Pd/Al_2O_3 > 1.1 wt% Pd/SiO_2 > 0.6 wt% Pd/Al_2O_3 > 0.3 wt% Pd/Al_2O_3, independent of the support and despite the substantial difference in acidity between Al_2O_3 and SiO_2.

With the HTR 0.3-wt% Pd/Al_2O_3 and 2.77-wt% Pd/Al_2O_3 samples that were pretreated with NH_3 before the 22DMB hydroconversion reaction, less CO_2 formed during the TPO (Fig. 5) than with the nontreated catalysts (Fig. 4). The difference was more pronounced for the low-loaded catalyst; specifically, half as much of CO_2 evolved during TPO of NH_3 pretreated 0.3 wt% Pd/Al_2O_3 compared to that of the sample without NH_3 treatment (Fig. 5). The maxima of the rate of CO_2 evolution for the NH_3-pretreated HTR Pd/Al_2O_3 samples were shifted to lower temperatures in comparison with the HTR catalysts without NH_3 treatment.

3.4. Characterization of differently pretreated Pd/Al_2O_3 catalysts by temperature-programmed (palladium) hydride decomposition (TPHD)

The shapes of the TPHD spectra of the Pd/Al_2O_3 catalysts and the peak positions were affected by the pretreatment method and the metal weight loading (Fig. 6). The amount of H_2 liberated during TPHD was $\leqslant 0.03$ H atom per Pd_{bulk} atom for the LTR-pretreated samples with metal loadings of 0.3 and 0.6 wt%. For the same samples the H/Pd_{bulk} ratios were one order of magnitude higher after the HTR but 40–50% less after regeneration (Table 1). With metal loadings of 1.46 and 2.77 wt%, the amount of H_2 formed during TPHD was approximately the same, regardless of the catalyst pretreatment (Table 1). For all metal loadings the temperature of maximum H_2 release was $\sim 20\,^{\circ}C$ lower for HTR-pretreated samples than for LTR-pretreated samples. After regeneration the temperature of the maximum rate of β-PdH phase decomposition did not change significantly for the 1.46 wt% Pd/Al_2O_3 and 2.77 wt% Pd/Al_2O_3 catalysts but increased by $\sim 10\,^{\circ}C$ for the 0.3 wt% Pd/Al_2O_3 and 0.6 wt% Pd/Al_2O_3 catalysts as compared to the HTR samples. A summary of the temperatures associated with the maximum rate of β-PdH phase decomposition for different Pd/Al_2O_3 catalysts is shown in Fig. 7.

3.5. Characterization of differently pretreated Pd/Al_2O_3 catalysts by IR spectroscopy

The FTIR results showed that dehydroxylation occurs during HTR pretreatment of the 0.3 and 2.77 wt% Pd/Al_2O_3 catalysts as compared to the LTR-pretreated samples (Fig. 8). The intensity of all types of OH-groups decreased: mono- ($\sim 3770\ cm^{-1}$), di- (~ 3665, ~ 3680, and $\sim 3730\ cm^{-1}$), and tri-coordinated ($\sim 3600\ cm^{-1}$) hydroxyls [20,21]. As well, a new monocoordinated hydroxyl band was present at

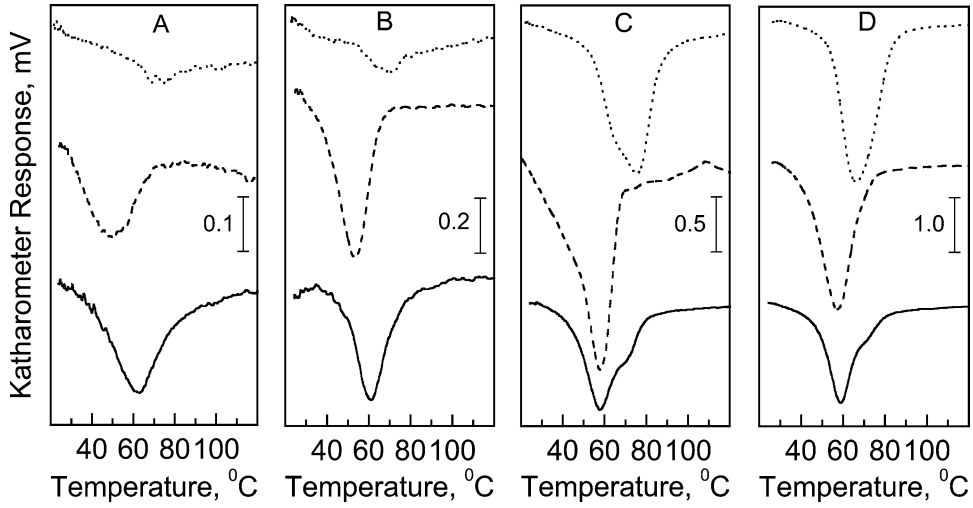

Fig. 6. TPHD profiles of 0.3 wt% Pd/Al_2O_3 (A), 0.6 wt% Pd/Al_2O_3 (B), 1.46 wt% Pd/Al_2O_3 (C), and 2.77 wt% Pd/Al_2O_3 (D) catalysts subjected to the LTR (dotted lines), HTR (dashed lines), and regeneration (solid lines) pretreatment protocols. To facilitate a comparison of H/Pd_{bulk} values (integrated areas within respective negative peaks) for differently metal-loaded catalysts, scales of the y-axis are adjusted to correlate with Pd loading.

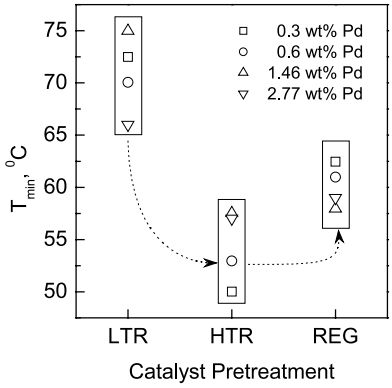

Fig. 7. Peak minimum location in the TPHD profiles of differently pretreated Pd/Al_2O_3 catalysts.

$\sim 3795\ cm^{-1}$. In fact, the HTR pretreatment decreased the Brønsted acidity of the catalyst surface, because the deprotonation energy decreases in the order mono- > di- > tricoordinated OH-groups [20,21] and the relative decrease in intensity upon the HTR is larger for the multicoordinated hydroxyls than for the monocoordinated hydroxyls (Fig. 8). Regeneration, which produces water via the reduction of PdO, resulted in the regeneration of the hydroxyl groups, albeit the band intensities were lower than in case of the LTR samples. In addition, the regenerated samples had a higher fraction of monocoordinated hydroxyls in comparison with the LTR samples (Fig. 8). Thus, the Brønsted acidity of the samples subjected to regeneration was lower than that of the samples after LTR; however, the Brønsted acidity of the regenerated samples was higher than that of the HTR samples. The narrow band at 3598–3610 cm^{-1} that is present after regeneration, especially for the 0.3 wt% sample (Fig. 8), may be attributed to both tricoordinated hydroxyl and OH-stretching vibrations (B_1) in a hydroxycarbonate species [22]. Exposure of the samples to 80 Torr of CO for 16 h at ambient temperature increased the intensity of the band 3598–3610 cm^{-1} (not shown). Carbon monoxide exposure also decreased the intensity of the band at $\sim 3770\ cm^{-1}$ for all samples (not shown). This decrease could be the result of the water-gas shift reaction in which CO reacts with OH-groups to form CO_2 (or carbonates) and H_2O.

The results of CO adsorption on the 0.3 wt% Pd/Al_2O_3 and 2.77 wt% Pd/Al_2O_3 catalysts in the vibrational range of 1700–2300 cm^{-1}, are shown in Figs. 9–11. The carbonate vibration region (1200–1700 cm^{-1}) is shown in Fig. 12. Prior to describing the dynamics of the band intensity as a function of catalyst pretreatment, CO pressure, and exposure time, it is reasonable to summarize the band assignments.

The bands in the range of 2200–2240 cm^{-1} are usually attributed to CO adsorbed on coordinatively unsaturated Al^{3+}

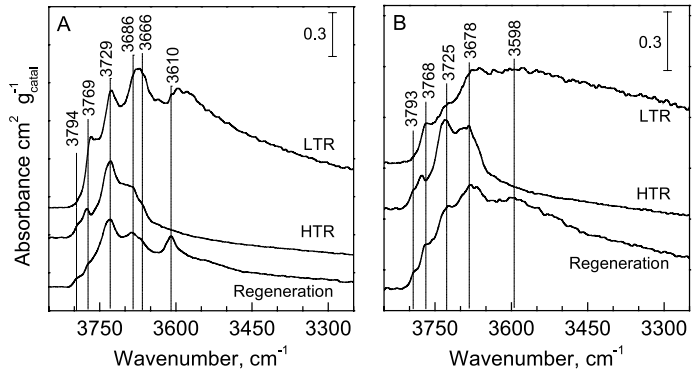

Fig. 8. FTIR spectra of the OH-stretching vibrational region of differently pretreated 0.3 wt% Pd/Al_2O_3 (A) and 2.77 wt% Pd/Al_2O_3 (B) catalysts.

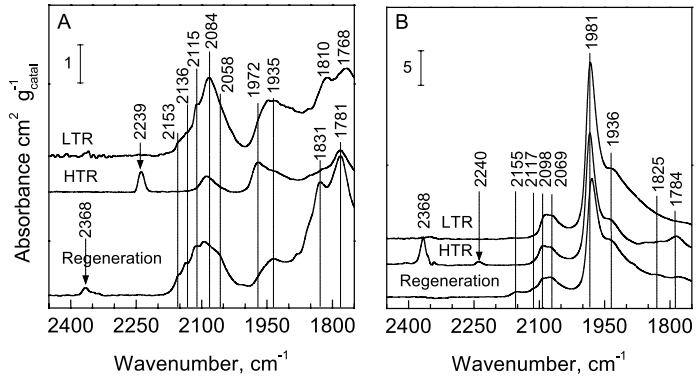

Fig. 9. FTIR spectra of CO adsorbed on differently pretreated 0.3 wt% Pd/Al_2O_3 (A) and 2.77 wt% Pd/Al_2O_3 (B) catalysts. After exposure to CO ($P_{CO} = 10$ Torr) at ambient temperature for 10 min the cell was evacuated for 10 min.

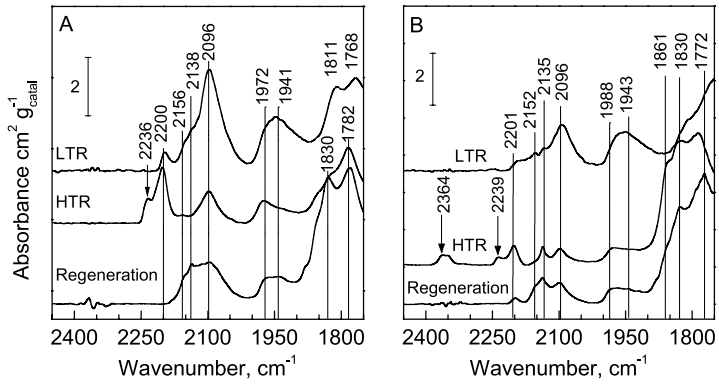

Fig. 10. FTIR spectra of CO adsorbed on the 0.3 wt% Pd/Al_2O_3 after exposure of the catalyst wafer to 80 Torr CO at ambient temperature for 10 min (A) and 16 h (B). The spectra were collected in the presence of gas phase.

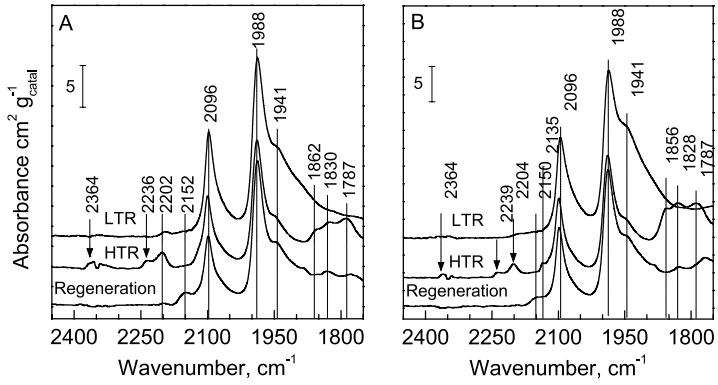

Fig. 11. FTIR spectra of CO adsorbed on the 2.77 wt% Pd/Al_2O_3 after exposure of the catalyst wafer to 80 Torr CO at ambient temperature for 10 min (A) and 16 h (B). The spectra were collected in the presence of gas phase.

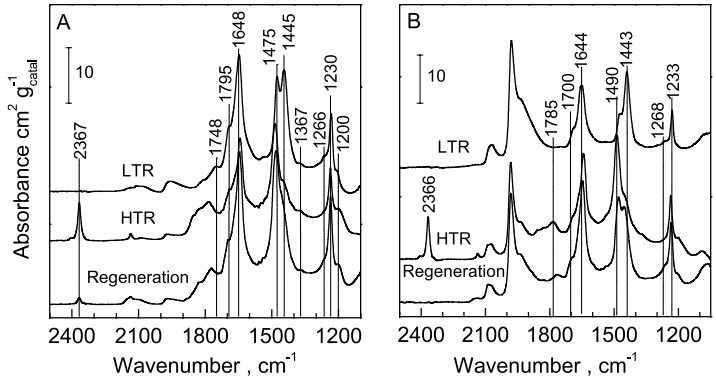

Fig. 12. FTIR spectra of the surface carbonate species vibrational region of differently pretreated 0.3 wt% Pd/Al_2O_3 (A) and 2.77 wt% Pd/Al_2O_3 (B) catalysts after exposure of the catalyst wafer to 80 Torr CO at ambient temperature for 16 h followed by evacuation.

ions [20,21,23]. The band in the range 2200–2204 cm^{-1} (Figs. 10, 11) is assigned to CO adsorbed on coordinatively unsaturated Al^{3+} ions in octahedral coordination, Al^{3+}_O [20, 21,23], and the band at 2236–2240 cm^{-1} (Figs. 9–11) is attributed to CO adsorbed on coordinatively unsaturated Al^{3+} ions in tetrahedral coordination, Al^{3+}_T [20,21,23]. The Al^{3+}_T species is considered to be a stronger Lewis acid than Al^{3+}_O [20,21,23], and, thus, it is more difficult to release CO from Al^{3+}_T by evacuation at room temperature (Fig. 9). The band at $\sim 2360\ cm{-}1$ (Figs. 9–12) is assigned to CO_2 bonded to strong Lewis sites of alumina [24]. This band is more pronounced for the evacuated samples than when CO was in the gas phase (Fig. 12).

The IR bands in the range of 2060–2100 cm^{-1} have been assigned to linear CO-Pd^0 species, and the bands in the

1750–2000 cm^{-1} range have been assigned to bridged and multi-bonded CO on Pd^0 [23,25–33]. However, no general agreement exists concerning the assignment of CO bands in the range of 2110–2160 cm^{-1} [25–33]. For purposes of this investigation it was assumed that the band at 2152–2156 cm^{-1} (Figs. 9–11) is assigned to CO adsorbed on Pd^{2+} ions [23,33], and the band at 2115 cm^{-1} (Fig. 9) is assigned to CO adsorbed on highly dispersed $Pd^{\sigma+}$. The band at 2135–2138 cm^{-1}, which is clearly seen in the spectra of adsorbed CO on the Pd/Al_2O_3 catalysts regardless of the CO pressure and exposure time (Figs. 9–11), has not been reported previously in the literature for the alumina-supported Pd. However, a similar vibrational frequency was reported for CO adsorbed onto Pd-Y (CO/Pd^+, 2140 cm^{-1} [23]) and Pd-MOR (CO/$Pd^{\sigma+}$, 2133 cm^{-1} [33]). Thus, it is reasonable to conclude that the band at 2135–2138 cm^{-1} is associated with CO adsorbed on Pd^+ ions incorporated into the alumina matrix.

The intensity of the bands of adsorbed CO depended on the CO pressure during adsorption and an exposure time. For example, the band at 2200–2204 cm^{-1} was observed only in the presence of gas-phase CO and was absent after evacuation (compare the spectra for HTR samples in Fig. 9 with those in Figs. 10, 11). Also the intensity of the bands at 2135–2138 and 2360 cm^{-1} increased with exposure time (Figs. 10 and 11). The largest increase in intensity with CO exposure time was observed for the bands at 2060–2100 cm^{-1} of the linear modes of CO adsorbed on Pd. This change is most apparent for the 2.77 wt% Pd/Al_2O_3 (Figs. 9 and 11).

The main differences between the FTIR spectra of adsorbed CO for the HTR and the LTR Pd/Al_2O_3 catalysts were that the HTR resulted in new bands at 2236–2240, ∼ 2360, and 2135–2138 cm^{-1} and in an intensity increase of the band at 2200–2204 cm^{-1} (Figs. 10 and 11). As well, the bands at 2152–2156 and 2115 cm^{-1} disappeared, and the bands of CO adsorbed on Pd^0 decreased in intensity significantly.

After regeneration of the Pd/Al_2O_3 catalysts the bands at 2152–2156 and 2115 cm^{-1} reappeared (Figs. 9–11), and the band at 2200–2204 cm^{-1} decreased in intensity. Regeneration also resulted in the disappearance of the bands at 2236–2240 and ∼ 2360 cm^{-1}. In addition, the band at 2135–2138 cm^{-1} became more pronounced (Figs. 9 and 10). For the 2.77 wt% Pd/Al_2O_3 catalyst this band was encompassed by the more intense bands at 2150–2155 cm^{-1} and 2117 or 2096 cm^{-1} (Figs. 9B and 11). In fact, deconvolution of the spectra for 2.77 wt% Pd/Al_2O_3 after regeneration (not shown) indicated that at least one more band was present between the bands at 2155 and 2117 cm^{-1} (Fig. 9B) and between the bands at ∼ 2050 and 2096 cm^{-1} (Fig. 11). Last, regeneration resulted in an increase in intensity of the bands characteristic of CO adsorbed on the Pd^0 sites. However, the intensities of these bands were still lower than those for the LTR samples.

After an extended interaction of CO with the 0.3 and 2.77 wt% Pd/Al_2O_3 catalysts at 20 °C, intense bands appeared in the range of 1200–1700 cm^{-1}, the range for carbonate species (Fig. 12). The carbonate bands were most intense for the regenerated samples and least intense for the HTR 0.3 wt% Pd/Al_2O_3 and for the LTR 2.77 wt% Pd/Al_2O_3.

4. Discussion

Earlier kinetics investigations showed that the catalytic performance of Pd/Al_2O_3 for both nH and 22DMB hydroconversion is altered significantly by the type of catalyst pretreatment [3–5]. The idea was put forth that the role of the alumina support is not limited to maintaining a high dispersion of Pd. Rather, the surface acidity of the alumina increases substantially during the HTR catalyst pretreatment, and the acidity plays a decisive role in the catalysis of alkane conversion. A corollary to this idea is the idea that the Pd-catalyzed chemistry is overshadowed by the activity of activated alumina.

The impact of the alumina support on alkane conversion reactions is apparent when the catalytic performance of silica- and alumina-supported Pd is compared. After reduction at 300 °C there is little difference in the performance of the silica- and alumina-supported Pd catalysts in nH and 22DMB hydroconversion [34]. After HTR the Pd/SiO_2 is highly selective toward isomerization. However, the overall activity is much lower than for the LTR state, and the selectivity enhancement occurs at the expense of hydrogenolysis [35,36]. Silica has no acidity, and the HTR pretreatment of Pd/SiO_2 results in the formation of Pd silicide(s) [35,36]. In the case of Pd/Al_2O_3 catalysts not only is the isomerization selectivity higher after HTR, but also the overall activity is increased. A further understanding of the decisive role of support acidity in alkane hydroconversion reactions will be developed from a consideration of the present results.

4.1. Pd/Al_2O_3 after low-temperature reduction

The LTR catalyst results serve, essentially, as a basis for comparison. The metal dispersion is low after LTR for the Pd/Al_2O_3 catalyst with the lowest metal loading (0.3 wt%) in comparison with the other Pd/Al_2O_3 samples (23% vs 29–39%, Table 1). It is unlikely that the same preparation method leads to larger particles when less catalyst precursor is deposited. Rather, the characterization methods are unsatisfactory for determining metal particle size in very low-metal-loaded Pd/Al_2O_3 samples. It is difficult to differentiate between XRD patterns that originate from the metal and from the support [37]; the contrast of small Pd particles is low in HRTEM micrographs; and the small Pd particles may have a different stoichiometry of H_2 adsorption than the larger particles, especially if the Pd in the particles is not

fully reduced. The FTIR results for adsorbed CO are consistent with the last suggestion. There is a vibrational band at 2115–2117 cm^{-1} (Fig. 9) that has been attributed to CO adsorbed onto $Pd^{\sigma+}$ species [23,38–43] formed from the interaction between very small Pd particles and γ-alumina. The frequency of this band is substantially closer to the vibrational band of CO in the gas phase (2143 cm^{-1}) than the characteristic vibrations of CO bonded to zerovalent Pd species (1750–2100 cm^{-1}); this suggests a weaker interaction of CO with the Pd. Similarly, the other adsorbate used in metal dispersion measurements, hydrogen, may also be more easily displaced from $Pd^{\sigma+}$ sites than H atoms irreversibly bonded to zerovalent Pd species. The small hydrogen uptake associated with PdH formation with the 0.3 and 0.6 wt% Pd/Al_2O_3 catalysts (Table 1) is also consistent with the presence of very small metal particles in low-metal-loaded Pd/Al_2O_3 [44].

When the current kinetics results are presented in terms of moles of reacted alkane per gram of Pd per second, a comparison can be made with the work of Le Normand et al. [45] for C_6-alkane conversions over different Pd/Al_2O_3 catalysts subjected to reduction at $\leqslant 400\,^{\circ}C$. The overall activity results shown in Fig. 1 for the 2,2-dimethylbutane and *n*-hexane reactions are in very good agreement with the activities of the Pd/Al_2O_3 samples tested in methylcyclopentane and 2-methylpentane conversions presented in Ref. [45]. As expected for the LTR-pretreated Pd catalysts, alkane hydrogenolysis predominates over isomerization (Fig. 1, Table 2). This behavior is consistent with a mechanism for the LTR samples that is "metallic" in character.

4.2. Pd/Al_2O_3 after high-temperature reduction

There are a number of factors which support the idea that the mechanism of the reaction catalyzed by samples subjected to the HTR is "acidic" in character. First, there is a substantial enhancement in the overall activity and isomerization selectivity when the HTR pretreatment is used instead of the LTR (Fig. 1, Table 2, steady-state values). Even though for nH conversion the higher steady-state activity of the HTR samples is a result of less deactivation with time on stream as compared to the LTR samples [4], in the case of 22DMB conversion the HTR samples are more active even at the initial stage of the reaction [4]. Second, for the HTR alumina-supported Pd catalysts the activity per gram of catalyst is either independent of (nH hydroconversion) or has a very weak dependence on the Pd loading (22DMB hydroconversion) [4]. Last, the substantial difference in the activation energies for 22DMB isomerization catalyzed by HTR ($\sim$ 20 kcal/mol) and LTR ($\sim$ 50 kcal/mol) Pd/Al_2O_3 samples [4] is indicative of different reaction mechanisms.

The acid-catalyzed mechanism involves the participation of Lewis acid sites of γ-alumina activated by HTR [2–4]. Strong Lewis acid sites of aluminas will activate paraffins [46]. However, isomerization, the predominant reaction pathway for the HTR samples, does not occur on metal-free (HTR) alumina samples. Thus, Pd is required mainly (but not exclusively) to supply H atoms to spill over onto the acid sites of Al_2O_3. This role of Pd is further demonstrated by the results of *n*-hexane conversion without H_2 in reaction mixture (H_2 was replaced by Ar carrier gas) catalyzed by 1.46 wt% Pd/Al_2O_3 (HTR) at 290 °C. Very few C_6-isomers form after 3 min of reaction with a conversion of $\sim$ 0.3%. Instead, olefin formation, mainly hex-1-ene, is predominant ($\sim$ 3% conversion). After 2.5 h on stream the catalyst lost nearly all its initial activity and no C_6-isomer alkanes formed. Thus, H_2 and metal are both required for isomerization even though the reaction occurs mainly on acid sites of the support. The same molecular-level description appears to be appropriate for alumina-supported Pt subjected to HTR. However, Pt is much more active than Pd for alkane conversion reactions, and the contribution of the acidic pathway is less pronounced [5].

The conclusion that alkane activation proceeds on the strong Lewis acid sites of alumina agrees well with the "carbenium" mechanism proposed by Kazansky et al. [46]. However, without excess H atoms alkane activation leads to dehydrogenation and coke formation. Therefore, the mechanism of alkane isomerization over the HTR samples involves alkane activation on alumina with subsequent carbenium ion formation. The carbenium ions form by hydride abstraction from the alkane either by a protonic form of spilt-over hydrogen [47] or by a Lewis acid site.

The classic dual-function mechanism with alkene formation on the metal and isomerization at an acid site cannot be excluded. However, there are some indications that the dual-function mechanism plays a less important role for HTR samples. For example, at the relatively low reaction temperature (290 °C) and high H_2 pressure used in this work, the calculated equilibrium partial pressures of olefins (hex-1-ene from nH and 3,3-dimethylbut-1-ene from 22DMB) are very low, $\sim 6\times10^{-4}$ and $\sim 5\times10^{-6}$ Torr, respectively [48]. Similar suggestions, based on changes in the reaction temperature and hydrogen partial pressure, have already been raised by others against the intermediacy of olefinic species and the classical dual-function mechanism [49–52]. Nevertheless, we would like to emphasize that HTR of Pd/Al_2O_3 leads to a significant increase in isomerization activity, associated with rearrangement of carbenium ions on acid sites of alumina, regardless of how these ions are formed.

The importance of support acidity is clearly observed in the results with Ni/Al_2O_3. When Ni/Al_2O_3 pretreated by HTR catalyzes the conversion of 22DMB, the selectivity toward isomerization products is $\sim$ 7% (Fig. 3). With Ni/SiO_2 [11] and Ni powder [12–14], neither of which possesses Lewis acid sites, no isomerization chemistry takes place; hydrogenolysis occurs with 100% selectivity. The modest level of isomerization selectivity of the HTR Ni/Al_2O_3 compared to the behavior of HTR Pd samples may result from two reasons. First, the surface of the HTR Ni may contribute more to the overall catalytic activity than acid sites of active alumina—even if the Ni was decorated by alumina species

[53,54]. Second, only a relatively small fraction of Lewis acid sites of HTR alumina may participate in alkane activation. As the sample was a physical mixture of 0.0019 g of 5 wt% Ni/Al_2O_3 and 0.2536 g of Al_2O_3, the majority of the Al_2O_3 was in loose contact with Ni. Under such conditions hydrogen spillover would not effectively provide active hydrogen to acid sites of the vast majority of admixed Al_2O_3. Regeneration of the HTR Ni/Al_2O_3 significantly decreases the Lewis acidity of Al_2O_3 (Section 3.5), and correspondingly the isomerization selectivity of Ni/Al_2O_3 is negligible (Fig. 3).

As would be expected when catalyst acidity is important, catalytic performance is affected by the preadsorption of NH_3. Ammonia selectively neutralizes the acid centers, because the strongly bound NH_3 is associated with the Al_2O_3 rather than the metal sites [10]. Indeed, NH_3 is completely removed from the surface of Pd(100) at temperatures below 80 °C [55]. Furthermore, the removal of the last NH_3 ligand from a silica-supported $Pd(NH_3)_4^{2+}$ complex takes place at ∼ 250 °C [56], well below the temperature of 22DMB conversion (290 °C). Accordingly, Fig. 2 shows that the catalytic behavior of 0.3- and 2.77-wt% Pd/Al_2O_3 HTR samples precovered with NH_3 is very different than the HTR samples that were not treated with NH_3. The NH_3 pretreatment significantly suppresses both the isomerization selectivity and the activity of the HTR catalysts. In fact, the NH_3-pretreated samples are even less active than the LTR samples.

The presence of acid sites on activated Al_2O_3 was established by the FTIR study of adsorbed CO on 0.3 and 2.77 wt% Pd/Al_2O_3 catalysts subjected to HTR (Figs. 9–11). Carbon monoxide chemisorption on γ-Al_2O_3 is characterized by three IR bands: $(CO)_A$ at 2195–2210 cm^{-1}, $(CO)_B$ at 2215–2220 cm^{-1}, and $(CO)_C$ at 2235–2240 cm^{-1} [21]. The strongest Lewis acid sites manifest themselves by the presence of the $(CO)_C$ band associated with exposed *cus* Al_T^{3+} ions, most likely located in crystallographically defective configurations. For the HTR samples these strongest acid sites are detectable after a short exposure to CO and evacuation (Fig. 9). Their appearance is often correlated with the presence of OH species with a vibrational frequency of 3775 cm^{-1} (Fig. 8) [21]. In case of the HTR-pretreated 0.3- and 2.77-wt% Pd/Al_2O_3 samples both the Al_T^{3+} and Al_O^{3-} species are present. With the LTR and regenerated samples, only Al_O^{3+} species are present (Figs. 10 and 11).

Carbon monoxide adsorption also results in the formation of surface carbonates (Fig. 12). The carbon dioxide required to form the carbonates is likely produced via CO disproportionation or water-gas shift reaction with OH groups of Al_2O_3. The former process proceeds on small Pd particles [57], whereas both mechanisms may operate on alumina [58]. The linearly bonded CO_2 with a vibrational frequency of 2360–2373 cm^{-1} is a signature of the strongest Lewis acid sites [24]. This band is located at 2364–2367 cm^{-1} in the spectra of HTR samples after CO adsorption, and it is absent in the spectra of the LTR and regeneration samples (Figs. 9–12). The adsorption of CO_2 on alumina is also accompanied by the formation of characteristic bands of carbonates at 1760–1835 cm^{-1} and 1190 cm^{-1} and a supplementary band at 1790 cm^{-1} [21]. The presence of the bicarbonate species (B_1) is manifested by strong ν_{CO} bands at ∼ 1650 cm^{-1} and ∼ 1440 cm^{-1}, by a δ_{OH} band at ∼ 1230 cm^{-1}, and by a ν_{OH} band at ∼ 3618 cm^{-1} [22]. Upon high-temperature treatment another bicarbonate (B_2) species forms at the expense of the B_1 species [22,24]. The two bicarbonate species are distinguishable by the position of the symmetric ν_{OCO} mode: ∼ 1440 cm^{-1} for B_1 and ∼ 1480 cm^{-1} for B_2. The B_2 species forms mostly at the expense of the basic (reactive) OH species at 3775 cm^{-1}. The relatively low B_2/B_1 ratio observed for LTR samples increases after HTR and then decreases after regeneration (Fig. 12). Thus, the dynamics of the carbonate band intensities reflects the changes in acid–base properties of differently pretreated Pd/Al_2O_3 catalysts.

While the presence of stronger Lewis acid sites in HTR samples of Pd/Al_2O_3 is clear, the state of the Pd particles requires further clarification. The intensity of the CO–Pd bands for the 0.3 wt% Pd/Al_2O_3 HTR sample is considerably less than the respective bands for LTR and regenerated samples (Fig. 9). The intensity difference cannot be attributed to a change in the metal surface area, as discussed in the Section 4.1. Rather, the Pd particles on the Al_2O_3 support are altered by HTR. This suggestion gains substance by consideration of the TPDH results (Figs. 6, 7). The β-hydride decomposition temperature for all HTR-pretreated catalysts is ∼ 20–25 °C lower than the decomposition temperature of the LTR samples. This behavior is reminiscent of the difference in the decomposition temperature of β-hydride phases of Pd and PdAl alloys; the hydride of $Pd_{0.97}Al_{0.03}$ foil is less stable than that of pure Pd [59,60]. Therefore, the Pd/Al_2O_3 catalysts may undergo a partial transformation into a PdAl alloy when reduced at 600 °C. This suggestion agrees well with the conclusions drawn from an earlier XRD study of Pd/Al_2O_3 catalysts [1,61].

The fact that no Pd–Al alloy phase was detected by XRD for the Pd catalysts with metal loading less than 3 wt% and reduction time of 17 h is reasonable in the context of prior research. Kępiński et al. showed that reduction of 5 wt% Pd/Al_2O_3 at 700 °C for 40 h leads to the formation of 6 at.% Al in Pd ($Pd_{0.94}Al_{0.06}$); $Pd_{0.9}Al_{0.1}$ forms under more severe reduction conditions (800 °C for 40 h) [61]. Similarly, after prolonged (33 h) reduction at 600 °C, Al is present in the Pd phase of a 10 wt% Pd/Al_2O_3 catalyst [1]. However, Al incorporation was not detected by XRD when the reduction time was 17 h [1]. The amount of Al in the Pd was below the detection limit. Indeed, available XRD data for the Pd–Al bulk system indicate that the lattice parameter decreases by 4×10^{-4} nm for the $Pd_{0.975}Al_{0.025}$ and 7×10^{-4} nm for the $Pd_{0.95}Al_{0.05}$ [59], and by 4×10^{-4} nm for the $Pd_{0.97}Al_{0.03}$ [62], compared to pure Pd. For the (111) reflection these changes in lattice parameter correspond to the shift of a few hundredths of a degree in 2θ. Such a small shift cannot

be detected for highly dispersed Pd/Al_2O_3 catalysts of relatively low metal loading, the XRD patterns of which contain low-intensity, broad Pd lines overlapping with reflections of the γ-Al_2O_3 support [37].

Similar detection problems are characteristic of other spectroscopic techniques such as XPS and EXAFS. The Pd core level shifts in XPS spectra associated with alloying are usually very small and metal particle size dependent. The signal from Al incorporated into a Pd–Al alloy is typically too weak to delineate it from the background signal of the Al in the support for both XPS and Al*K*-edge EXAFS spectra. Aluminum is a much weaker scatterer of electrons than Pd, and thus the Pd–Pd coordination will dominate in the Pd*K*-edge EXAFS spectra.

4.3. Pd/Al_2O_3 after regeneration

Any Pd–Al alloy formed during HTR will be converted into PdO and Al_2O_3 by oxidation at 500 °C for 1 h. The subsequent 300 °C reduction step of the regeneration restores the Pd/Al_2O_3 state. This description is most appropriate for nanosized particles for which it is reasonable to assume a "complete conversion" during each step. It was shown previously [61] that oxidation at 500 °C for 5 h of 10 wt% Pd/Al_2O_3 subjected to HTR (containing a $Pd_{90}Al_{10}$ phase of 16 nm (TEM) or 36 nm (XRD) particles) restores a "normal" lattice parameter of Pd and restores its ability to form Pd–C solid solutions.

The higher stability of the hydride phase formed with the regenerated Pd/Al_2O_3 samples may indicate that the HTR Pd/Al_2O_3 samples are not oxidized completely during the first step of the regeneration (oxidation at 500 °C for 1 h). The distinctive shape of TPHD profiles of regenerated 1.46- and 2.77-wt% Pd/Al_2O_3 samples reflects the incomplete oxidation. In fact, TPHD traces for these catalysts show the decomposition of the β-hydride from two phases (Figs. 6(c) and 6(d), bottom profiles). Similar results were obtained with partly reoxidized PdAl foils [60]. Namely, the hydrogen isotherms of $Pd_{0.97}Al_{0.03}$ pretreated in air at 800 °C for 12 h showed the presence of two plateaus, which is consistent with incomplete oxidation [60]. A more drastic oxidation procedure (1000 °C for 24 h) was needed for complete oxidation [60]. Even if some residual PdAl alloy is present in the regenerated Pd/Al_2O_3 catalysts, it is unlikely that the unoxidized Al species are present at the particle surface because exposed Al atoms are easily oxidized by oxygen. Nevertheless, the surface properties of the regenerated samples are not the same as those of LTR samples.

The high isomerization selectivity for the regenerated samples in comparison with the LTR can be related to a difference in state of the metal particles and their interaction with alumina. It is proposed that oxidation of the Pd–Al alloy (formation of which during HTR is hypothesized in a previous section) leads to formation of small Al_2O_3 clusters on (and in) Pd particles. Partial coverage of Pd by small Al_2O_3 clusters splits the multiple Pd ensembles, which should inhibit the ensemble size demanding reactions such as metal-catalyzed hydrogenolysis. A closer examination of the TOF data for hydrogenolysis (Table 2, $TOF_{<C6}$) for LTR and regenerated samples indicates that, in fact, such an effect does exist in the case of 22DMB reaction; regenerated samples except the 0.3 wt% Pd/Al_2O_3 are less active for hydrogenolysis than the LTR samples. The unusual behavior of the 0.3 wt% Pd/Al_2O_3 sample needs further investigation; however, it is plausible that the very low metal dispersion (1%) for the regenerated catalyst measured by H_2 chemisorption (Table 1) is attributed to experimental error, most likely a significant underestimation.

A similar comparison of LTR and regenerated samples for the nH reaction shows that the 0.6-wt% and 1.46-wt% regenerated samples are more active for hydrogenolysis than the LTR catalysts, whereas the 0.3-wt% sample showed a much higher hydrogenolysis activity in the regenerated state (similarly as for 22DMB reaction). In fact, only the regenerated 2.77-wt% Pd/Al_2O_3 catalyst exhibit lower hydrogenolysis activity than the LTR sample. If the 0.3-wt% sample is considered as a special case, it can be concluded that changes in the hydrogenolysis activity in the nH hydroconversion reaction that result from the LTR–HTR–regeneration pretreatment are small. It must be recalled that, in general, Pd is a poor catalyst for hydrogenolysis compared to other noble metals. In addition, Pd is usually much less structure sensitive for alkane hydrogenolysis than other noble metals [45, 63].

More importantly, regeneration of Pd/Al_2O_3 results in a high activity toward isomerization compared to that of the LTR samples (Table 2 and Fig. 1). This behavior is observed for all catalysts used in both reactions, but it is more apparent for the low loaded samples (0.3 and 0.6 wt%). Two possibilities should be considered: (i) some support acidity (gained during HTR) remains after regeneration and (ii) specific active sites on the surface of Pd particles are generated by the regeneration pretreatment. For the regenerated samples the role of the Lewis acid sites of activated alumina does not appear to be decisive. The FTIR results show that very few of Lewis acid sites are present after regeneration. The water formed during the oxidation–reduction treatment may suppress the Lewis acidity of the regenerated samples. As well, the substantial increase in the intensity of the CO band at the frequencies greater than 2100 cm^{-1} (Fig. 9) suggests some electronic changes in Pd species. Previously, such frequency shifts were interpreted in terms of partially electron-deficient Pd species [18–22,64]. The presence of these species in the regenerated samples, characterized by weaker CO–Pd bonding, may also be responsible for the increased isomerization (vs hydrogenolysis) selectivity and for the decrease in carbon deposition during nH and 22DMB hydroconversion reactions.

An abundant presence of Al_2O_3 species on the Pd surface (from oxidation of PdAl, formation of which upon HTR is proposed in a previous section), should enhance the interaction of Pd and Al_2O_3 in comparison with the LTR samples

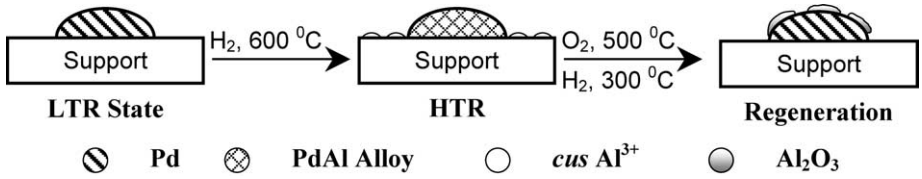

Fig. 13. Schematic representation of suggested changes in the state and morphology of the Pd/Al_2O_3 catalysts resulting from different pretreatments.

and contribute to evolution of catalytic behavior. A significant role of the Pd–Al interaction at the Pd–Al_2O_3 interface was confirmed by theoretical calculations [65]. As well, the importance of close proximity of Pt and Al_2O_3 sites in shifting product selectivity toward *n*-hexane in the hydroconversion of methylcyclopentane was emphasized earlier by the group of Kramer [10,66,67].

5. Conclusions

The structural and morphological changes of Pd and Al_2O_3 that occur when a Pd/Al_2O_3 catalyst is subjected to various pretreatments have been elucidated (Fig. 13). The HTR pretreatment substantially increases the strong Lewis acidity of the Al_2O_3. Based on the shift in the maximum temperature of the Pd hydride phase decomposition and the suppression of CO adsorption on Pd^0 sites, it was suggested that Pd–Al moieties also form during the HTR. The regeneration of the HTR catalysts decreases the Lewis acidity of the Pd/Al_2O_3 catalysts, probably because the Al_2O_3 surface is hydroxylated by H_2O formed during reduction of PdO. The shift in the temperature of the palladium hydride phase decomposition toward that of bulk Pd and the restoration of the ability of Pd to adsorb CO is consistent with the destruction of the Pd–Al alloy particles formed during the HTR and the concomitant formation of Al_2O_3 moieties located on the Pd surface. In addition, the FTIR spectroscopic results for CO adsorption provide evidence that Pd particles of the regenerated samples are electron deficient in comparison with the HTR Pd/Al_2O_3 catalysts.

The substantial increase in isomerization activity of the HTR Pd/Al_2O_3 for the nH and 22DMB hydroconversion reactions is explained by the participation of Al_2O_3 Lewis acid sites. This hypothesis is supported by the kinetics results, which show low isomerization selectivity when the support acidity is suppressed by adsorbed NH_3. Thus, the major role of Pd is to provide the dissociated hydrogen required for hydrogenative desorption of rearranged alkyl fragments from acid sites of γ-Al_2O_3. For the regenerated samples, the Al_2O_3 moieties located on the Pd surface probably interact with nearby palladium species, creating sites that are very active for alkane isomerization and, simultaneously, resistant to coking.

Acknowledgments

This work was supported in part by the Committee for Scientific Research of Poland (KBN) within Grant 4T09B 102 22 (supporting the PhD thesis of M.S.). J.L.d'I. and V.I.K. gratefully acknowledge support from the National Science Foundation (CTS 0086638) of the United States of America.

References

[1] W. Juszczyk, D. Łomot, Z. Karpiński, J. Pielaszek, Catal. Lett. 31 (1995) 37.
[2] D. Łomot, W. Juszczyk, Z. Karpiński, Appl. Catal. A 155 (1997) 99.
[3] M. Skotak, Z. Karpiński, Polish J. Chem. 75 (2001) 839.
[4] M. Skotak, D. Łomot, Z. Karpiński, Appl. Catal. A 229 (2002) 103.
[5] M. Skotak, Z. Karpiński, Chem. Eng. J. 90 (2002) 89.
[6] J.B. Peri, J. Phys. Chem. 70 (1966) 3168.
[7] H. Knözinger, P. Ratnasamy, Catal. Rev. Sci. Eng. 17 (1978) 31.
[8] M. Skotak, J. Kijeński, Z. Karpiński, Polish J. Chem. 77 (2003) 757.
[9] D. Łomot, W. Juszczyk, Z. Karpiński, F. Bozon-Verduraz, New J. Chem. 21 (1997) 977.
[10] H. Glassl, K. Hayek, R. Kramer, J. Catal. 68 (1981) 397.
[11] H. Matsumoto, Y. Saito, Y. Yoneda, J. Catal. 19 (1970) 101.
[12] H. Matsumoto, Y. Saito, Y. Yoneda, J. Catal. 22 (1971) 182.
[13] F.J. Schepers, E.H. van Broekhoven, V. Ponec, J. Catal. 96 (1985) 82.
[14] M.W. Vogelzang, M.J.P. Botman, V. Ponec, Faraday Discuss. Chem. Soc. 72 (1981) 33.
[15] J.P. Boitiaux, J. Cosyns, S. Vasudevan, in: Preparation of Catalysts III, Elsevier, Amsterdam, 1983, p. 123.
[16] M. Bonarowska, J. Pielaszek, V.A. Semikolenov, Z. Karpiński, J. Catal. 209 (2002) 528.
[17] S.S. Deshmukh, V.Yu. Borovkov, V.I. Kovalchuk, J.L. d'Itri, J. Phys. Chem. B 104 (2000) 1277.
[18] L. Marchese, M.R. Boccuti, S. Coluccia, S. Lavagnino, A. Zecchina, L. Bonneviot, M. Che, in: C. Morterra, A. Zecchina, G. Costa (Eds.), Structure and Reactivity of Surfaces, Elsevier, Amsterdam, 1989, p. 653.
[19] F. Garin, G. Maire, S. Zyade, M. Zauwen, A. Frennet, P. Zielinski, J. Mol. Catal. 58 (1990) 185.
[20] E.A. Paukshtis, Infrared Spectroscopy in Acid–Base Heterogeneous Catalysis, Nauka, Moscow, 1992.
[21] C. Morterra, G. Magnacca, Catal. Today 27 (1996) 497.
[22] C. Morterra, A. Zecchina, S. Coluccia, A. Chiorino, J. Chem. Soc. Farad. Trans. I 73 (1977) 1544.
[23] A.A. Davydov, Infrared Spectroscopy of Adsorbed Species on the Surface of Transition Metal Oxides, Wiley, Chichester, 1990.
[24] J.-C. Lavalley, M. Benaissa, G. Busca, V. Lorenzelli, Appl. Catal. 24 (1986) 249.
[25] G. Rupprechter, H. Unterhalt, M. Matthias, P. Galletto, L. Hu, H.-J. Freund, Surf. Sci. 502 (2002) 109.
[26] E. Ozensoy, D.C. Meier, D.W. Goodman, J. Phys. Chem. B 106 (2002) 9367.
[27] D. Stacchiola, A.W. Thompson, M. Kaltchev, W.T. Tysoe, J. Vac. Sci. Technol. A 20 (2002) 2101.

[28] R.S. Monteiro, L.C. Dieguez, M. Schmal, Catal. Today 65 (2001) 77.
[29] V.V. Kaichev, I.P. Prosvirin, V.I. Buhtiyarov, H. Unterhalt, G. Rupprechter, H.J. Freund, J. Phys. Chem. B 107 (2003) 3522.
[30] S.N. Reinfsnyder, M.M. Otten, H.H. Lamb, Catal. Today 39 (1998) 317.
[31] K. Wolter, O. Seiferth, J. Libuda, H. Kuhlenbeck, M. Bäumer, H.-J. Freund, Surf. Sci. 402–404 (1998) 428.
[32] K. Wolter, O. Seiferth, J. Libuda, H. Kuhlenbeck, M. Bäumer, H.-J. Freund, Chem. Phys. Lett. 277 (1997) 513.
[33] Z. Zhang, W.M.H. Sachtler, J. Mol. Catal. 67 (1991) 349.
[34] D. Łomot, W. Juszczyk, J. Pielaszek, Z. Karpiński, Polish J. Chem. 69 (1995) 1551.
[35] W. Juszczyk, Z. Karpiński, J. Catal. 117 (1989) 519;
W. Juszczyk, Z. Karpiński, J. Pielaszek, J.W. Sobczak, New J. Chem. 17 (1993) 573.
[36] W. Juszczyk, Z. Karpiński, D. Łomot, J. Pielaszek, J. Catal. 220 (2003) 299.
[37] R.K. Nandi, R. Pitchai, S.S. Wong, J.B. Cohen, R.L. Burwell Jr., J.B. Butt, J. Catal. 70 (1981) 298.
[38] F. Figueras, R. Gomez, M. Primet, Adv. Chem. Ser. No. 121 (1973) 480.
[39] V.N. Romannikov, K.G. Ione, L.A. Pedersen, J. Catal. 66 (1980) 121.
[40] M.A. Martin, J.A. Pajares, L. Gonzalez-Tejuca, Z. Phys. Chem. 140 (1984) 107.
[41] A.L. Tarasov, A.A. Shvets, A.V. Zaitsev, V.B. Kazanskii, Kinet. Katal. 27 (1986) 1181.
[42] W. Juszczyk, Z. Karpiński, I. Ratajczykowa, Z. Stanasiuk, J. Zieliński, L.-L. Sheu, W.M.H. Sachtler, J. Catal. 120 (1989) 68.
[43] D. Tessier, A. Rakai, F. Bozon-Verduraz, J. Chem. Soc. Faraday Trans. 88 (1992) 741.
[44] M. Boudart, H.S. Hwang, J. Catal. 39 (1975) 44.
[45] F. Le Normand, K. Kili, J.L. Schmitt, J. Catal. 139 (1993) 234.
[46] V.B. Kazansky, V.Yu. Borovkov, A.V. Zaitsev, in: M.J. Phillips, M. Ternan (Eds.), Proceedings of the Ninth International Congress on Catalysis, Calgary, 1988, vol. 3, Chemical Institute of Canada, Ottawa, 1988, pp. 1426–1433.
[47] A. Zhang, I. Nakamura, K. Aimoto, K. Fujimoto, Ind. Eng. Chem. Res. 34 (1995) 1074.
[48] D.R. Stull, E.F. Westrum Jr., G.C. Sinke, The Chemical Thermodynamics of Organic Compounds, Wiley, New York, 1969.
[49] E. Iglesia, S.L. Soled, G.M. Kramer, J. Catal. 144 (1993) 238.
[50] H.Y. Chu, M.P. Rosynek, J.H. Lunsford, J. Catal. 178 (1998) 352.
[51] M. Steijns, G. Froment, Ind. Eng. Chem. Prod. Res. Dev. 20 (1981) 660.
[52] J.C. Duchet, D. Guillaume, A. Monnier, C. Dujardin, J.P. Gilson, J. van Gestel, G. Szabo, P. Nascimento, J. Catal. 198 (2001) 328.
[53] R. Lamber, G. Schultz-Ekloff, Surf. Sci. 258 (1991) 107.
[54] J. Zieliński, J. Mol. Catal. 83 (1993) 197.
[55] C. Xu, D.W. Goodman, J. Phys. Chem. B 102 (1998) 4392.
[56] M. Bouchemoua, M. Che, D. Olivier, D. Delafosse, M. Kermarec, in: P. Barnet, L.C. Dufur (Eds.), Reactivity of Solids, in: Material Science Monographs, vol. 28B, Elsevier, Amsterdam, 1985, p. 1083.
[57] S. Ichikawa, H. Poppa, M. Boudart, J. Catal. 9 (1985) 1.
[58] N.D. Parkyns, J. Chem. Soc. A (1967) 1910.
[59] Y. Sakamoto, E. Kakahisa, Y. Kinari, Z. Phys. Chem. 179 (1993) 69.
[60] H. Noh, T.B. Flanagan, R. Balasubramanian, J.A. Eastman, Scr. Mater. 34 (1996) 863.
[61] L. Kępiński, M. Wołcyrz, J.M. Jabłoński, Appl. Catal. 54 (1989) 267.
[62] M. Ellner, J. Less-Common Met. 60 (1978) P15.
[63] Z. Karpiński, Adv. Catal. 37 (1990) 45.
[64] J. Zieliński, J. Chem Soc. Faraday Trans. 93 (1997) 3577.
[65] M. Kohyama, S. Kose, M. Kinoshita, R. Yamamoto, J. Phys. Chem. Solids 53 (1992) 345.
[66] R. Kramer, H. Zuegg, J. Catal. 80 (1983) 446.
[67] R. Kramer, H. Zuegg, in: Proceedings of the Eighth International Congress on Catalysis, Berlin, 1984, vol. 5, Dechema, Frankfurt-am-Main, 1984, p. 275.